Dual fiber spectrometer for highly non-degenerate entanglement source

Adam J. Fallon[a,b], Daniel R. Hart[a], Evan J. Katz[a], Brian E. Vyhnalek[a], Ian A. Chin[c], John D. Lekki[a]
[a]NASA Glenn Research Center, 21000 Brookpark Road, Cleveland, OH, USA 44135; [b]Oak Ridge Associated Universities, 100 ORAU Way, Oak Ridge, TN 37830, and [c]GRC-LERCIP, 21000 Brookpark Road, Cleveland, OH 44135

ABSTRACT

NASA is developing quantum metrology capabilities for potential space-based quantum components in future navigation and communications systems. Innate knowledge of component operation is key for the space qualification of these components. This paper focuses on the measurement and analysis of an important characteristic of an entanglement source, the joint spectrum. We describe a spectrometer based on dispersive optical fibers and present experimental measurements of the joint spectrum of a highly non-degenerate SPDC-based entanglement source that emits entangled photons in the near-infrared and telecommunications bands. How the analysis of such a joint spectrum could be applied to the modeling and simulation of entanglement swapping operations as possible extensions of quantum networks is examined. Lastly, we discuss how the separability of the two-photon state is quantified via Schmidt decomposition and how the degree of separability impacts the spectral purity of heralded single-photon emissions.

1. INTRODUCTION

Quantum entanglement is a fundamental process of quantum mechanics, where particles that are entangled have an intrinsic correlation that is not affected by their spatial separation. Quantum communication protocols take advantage of this phenomenon, among others, to connect links in quantum networks and transmit quantum information within network architectures [1]. The maturation of such networks will be critical for advances in quantum-secure communications, quantum sensor networks, and blind quantum computing [2]**.** These architectures typically consist of either optical fiber or free-space links. The former can use existing telecommunications infrastructure but has limited effective transmission distance due to the lack of robust quantum repeaters [3]. The latter can use space-based quantum assets to enable line-of-sight transmission over greater distances at the cost of needing to space-qualify and miniaturize quantum technologies. To aid in this effort, our research team at NASA Glenn Research Center is developing quantum metrology capabilities to characterize quantum network components and systems, the results of which are fed into high fidelity quantum models and simulations to estimate the performance of eventual real world quantum networks. We are further supporting the technology maturation of low size, weight, and power (low-SWaP) quantum devices for eventual integration into space-based quantum assets.

In this article, we discuss the measurement of the joint spectral intensity (JSI) of a low-SWaP time-energy entanglement source implemented in a periodically poled potassium titanyl phosphate (pp-KTP) waveguide that emits near-infrared (NIR) and infrared (IR) signal and idler photons, respectively. These desirable wavelengths provide flexibility for future applications both in deployment environment and choice of wavelength band as it is amenable to both free-space and fiber optic transmission. The source operates by spontaneous parametric down-conversion (SPDC), and, while the SPDC process has seen widespread adoption across academia and industry for generating entangled pairs of photons, there remain challenges in using these sources for quantum networks applications. One such example is that phase matching conditions in these sources can create unwanted spectral correlations that reduces their suitability for use in entanglement swapping architectures [4, 5] because such correlations reduce the indistinguishability of the entangled photons. Measuring the degree of this correlation involves finding the JSI of the entangled photons. Figure 1 illustrates this issue by showing simulated signal and idler spectra. Each spectrum was generated as a Gaussian distribution about central wavelengths 810 nm and 1550 nm, for signal and idler respectively. Entangled photon pairs can be spectrally correlated at various frequencies along idler and signal spectra. When a high degree of spectral correlation occurs, the output produces a 2D ellipse (Figure 1b). However, when the spectral correlation begins to vanish, the major and minor axes of the ellipse reduce

to a more circular form (Figure 1c). The latter is the pursued spectrum because it describes a system of two-photon states with a high degree of separability, which leads to useful, distinguishable Fock states, i.e., heralded single photons.

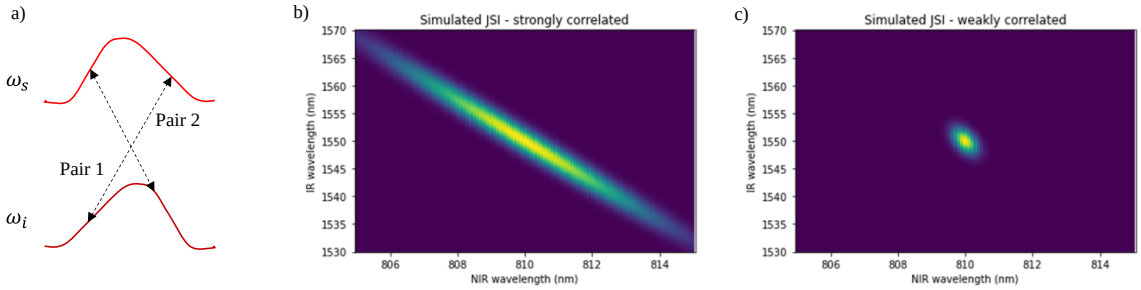

Figure 1: a) Shows how signal and idler photons can be correlated at different frequencies b) Joint Spectral Intensity of strongly correlated spectrum c) Joint Spectral Intensity of weakly correlated spectrum

The rest of this paper is organized as follows. In Section 2, we describe the dual fiber spectrometer setup we use to measure the JSI of this highly non-degenerate time-energy entanglement source, including the software required to extract the spectral information from the time-of-flight measurements at the core of the spectrometer. In Section 3, we develop the mathematical tools to quantitatively analyze the JSI of our entanglement source, and, as an initial test of our capabilities, we look at how spectral filtering alters the joint spectra by comparing the spectral purity for different combinations of spectral bandpass filters on the signal and idler photons. Finally, in Section 4, we conclude that dispersive fiber spectroscopy to measure the JSI can be a useful tool for analyzing multiple types of entangled photon pair sources, including highly non-degenerate sources, which will provide needed information to help inform future NASA mission decisions.

2. DUAL FIBER SPECTROMETER DESIGN AND OPERATION

Dispersive fiber spectroscopy is a common method for measuring the JSI of entangled photon pair sources by transforming spectral variations in the photons into time of arrival differences at the detectors [6]. The device under test, in the analysis presented here, is an SPDC-based time-energy entanglement source. This source utilizes a pulsed 532 nm pump laser to generate highly non-degenerate entangled photon pairs near 810 nm and 1550 nm. Our spectroscopy setup, as shown in Figure 2, differs from most implementations to date, in that it is based on two separate optical fibers acting as the dispersive media rather than a single common optical fiber [6, 7], or a chirped fiber Bragg grating [8]. The use of two fibers ensures similar total dispersion for the two highly non-degenerate photons while minimizing individual channel losses. We use optical fibers of lengths $L_{NIR} = 3.4$ km (780-HP) for the 810 nm photons and $L_{IR} = 29$ km (SMF-28e+) for the 1550 nm photons, which have dispersions of $\alpha_{NIR} = -130$ ps/(nm·km) and $\alpha_{IR} = 16$ ps/(nm·km), yielding total dispersions of $\alpha_{NIR}L_{NIR} = -440$ ps/nm and $\alpha_{IR}L_{IR} = 467$ ps/nm, respectively. The former is a calculated number based on the fiber length and dispersion information provided by the manufacturer [9]. The latter is calibrated using the time of arrival differences between the pulsed pump laser's RF timing reference output and its primary optical output, varied from 1540 nm to 1560 nm, after having transited the optical fiber. Based on the system timing jitter, we can expect spectral resolutions of 80 pm and 110 pm for the NIR and IR time of flight spectrometers, respectively.

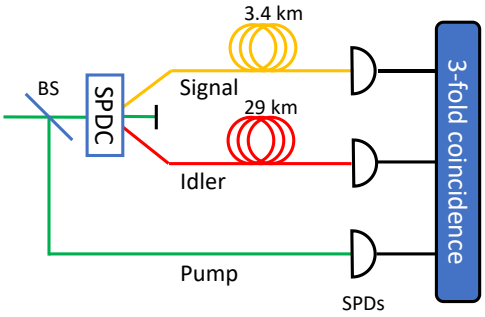

Figure 2: Schematic of the JSI setup. BS: beam splitter. SPDs: single photon detectors.

The JSI is recovered using time tags from the three-fold coincidence between the timing reference from the pump laser and detection of the entangled photon pair. The pump laser repetition rate exceeds the time tagger's maximum transfer rate; therefore, to avoid the associated buffer overrun, we include an artificial dead time in the laser timing reference, reducing the effective laser repetition rate as seen by the time tagger. While this solves the overrun issue, it also prevents tagging the specific pump pulse used in creating the detected entangled photon pair, an essential piece of information needed for generating the joint spectra. We recover some of the missing timing information with custom time tagging software. A timing diagram showing the general process can be seen in Figure 3. A coincidence measurement between the entangled photon pair starts the timing loop, where the limits on the coincidence window depend on the photon bandwidths and total fiber dispersions. The time stamps for the two photons, t_{NIR} and t_{IR} for the 810 nm and 1550 nm photons, respectively, are recorded and will be used in construction of the joint spectra. The software then records the time stamp of the next laser timing reference, t_p, which is delayed by a random integer multiple of the pump laser period. This closes the timing loop.

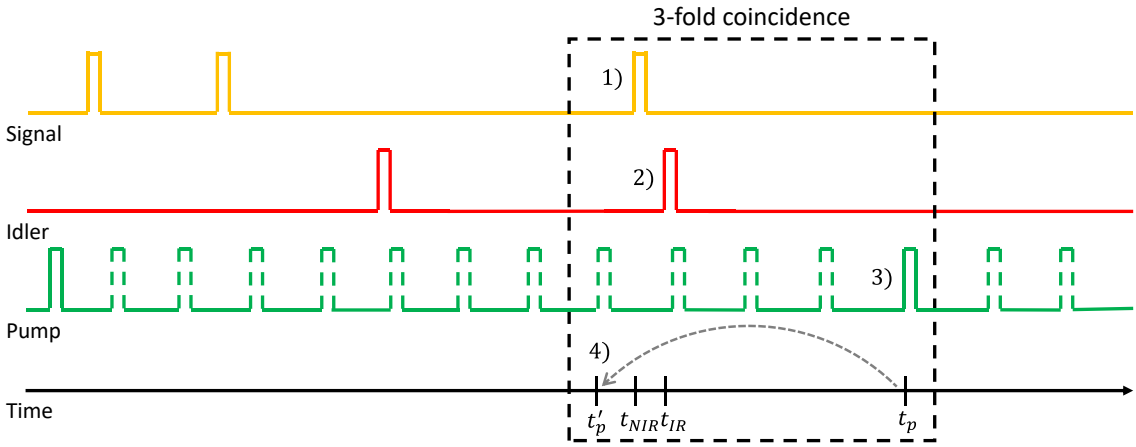

Figure 3: Timing diagram for detection of three-fold coincidence, recording of relevant time of arrivals, and recovery of pump pulse timing. 1) Detection of signal photon starts 3-fold coincidence timing loop. 2) Detection of idler photon within 20 ns coincidence window results in successful 2-fold coincidence. 3) The next pump laser timing reference is recorded to end 3-fold coincidence timing loop. Dashed lines show other pump laser timing references not recorded due to artificial dead time in time tagger. 4) Recover pump pulse reference time.

Generation of the JSI begins by calculating a modified pump pulse reference time, t_p', to give an absolute timing reference. Using the time stamps of the pump pulse reference and the 810 nm photon, which we use as the trigger photon starting the timing loop described above, and the modulo operation, t_p' is given by

$$t_p' = t_{NIR} - \left(t_{NIR} - t_p\right) \% \, \tau_p$$

where τ_p is the pump pulse period. From this, we generate the modified arrival times

$$t_i' = t_i - t_p',$$

for $i = NIR\ or\ IR$. The modified arrival times are then converted to wavelengths using the total fiber dispersion values and user-set wavelength bins. Finally, the 2D JSI histogram is generated from this wavelength data, examples of which are given in Figure 4. Because our time tagger is unable to resolve which specific pump pulse generates the photon pair, we introduce a restriction to this general method where the total variation in the time of arrival, Δt_i, of at least one of the entangled photons obeys

$$\Delta \mathrm{t}_i = \alpha_i L_i \Delta\lambda_i < \tau_p,$$

for the total dispersions, $\alpha_i L_i$, and the single photon bandwidths, $\Delta\lambda_i$. This restriction ensures that the measured photon pair was generated by a single pump pulse rather than leaving the possibility that the two photons originated during different pump pulses, which would affect the results of the JSI measurement. The inequality is satisfied in the presented configuration where $\Delta\lambda_{NIR} < 1.5$ nm, for all spectral filters used in the data presented here. This yields $\Delta t_{NIR} < 0.66$ ns, which is less than the pump period of $\tau_p = 2$ ns. An additional worry is that photons generated by neighboring pump pulses might fall within the two-photon coincidence window at the start of the timing loop and degrade the JSI. However, these spurious two-fold coincidences are suppressed by an additional factor of the photon pair generation rate, which is $\ll 0.001$ for the data presented here. These considerations become less relevant if the pump laser repetition rate is reduced.

3. CHARACTERIZATION OF NON-DEGENERATE PHOTON PAIRS AT 810 NM AND 1550 NM

To analyze the measured JSIs, we start by considering the two-photon states generated by the SPDC. These can be modeled by observing the interaction Hamiltonian of the nonlinear crystal,

$$\boldsymbol{H}_{Int} = \xi\left(\hat{a}_{NIR}^{\dagger}\hat{a}_{IR}^{\dagger} + H.c.\right),$$

where $\hat{a}_{NIR}^{\dagger}$ and $\hat{a}_{IR}^{\dagger}$are the creation operators for the signal and idler, respectively. There is no annihilation operator for the pump source because it is treated classically and is contained in the interaction strength, ξ, which is a function of the pump intensity and strength of the non-linearity. To calculate the output state from the crystal, we solve the Schrodinger equation for $\boldsymbol{H}_{Int}$. This gives us a unitary operator acting on the vacuum state,

$$\left|\psi_{out}\right\rangle = e^{-i/\hbar\xi\left(\hat{a}_{NIR}^{\dagger}\hat{a}_{IR}^{\dagger}+H.c.\right)t}\left|\ 0\right\rangle_{NIR}|0\rangle_{IR}.$$

When this output is expanded in a Taylor series, we obtain a superposition of states

$$|\psi_{out}\rangle \approx A_0|0\rangle_{NIR}|0\rangle_{IR} + A_1|1\rangle_{NIR}|1\rangle_{IR} + A_2|2\rangle_{NIR}|2\rangle_{IR} + \cdots,$$

where A_0, A_1, and A_2 are the amplitudes of vacuum state, two-photon state, 4-photon state, and so on respectively. This assumes that the correlation of the two-photon state is only related in photon number state $|n\rangle_{NIR}|n\rangle_{IR}$. In realistic systems, however, the photons emitted can be non-degenerate, have a continuum of spectral emission about the central signal and idler frequencies, $\omega_{NIR}\ and\ \omega_{IR}$, and, due to conservation of energy, be spectrally correlated. Discretization of the mode continuum will allow for quantitative examination of the two-photon states generated by the short pulses pumping the down conversion source. If we replace the singular photon states with electric field operators in the interaction Hamiltonian, we obtain

$$\boldsymbol{H}_{int}(x) = \int_{-\frac{x}{2}}^{\frac{x}{2}} \chi(x)\, E_p(x,t)\hat{E}_{NIR}(x,t)\hat{E}_{IR}(x,t)dx,$$

where $\chi(x)$ is the position dependent nonlinearity of the SPDC source, $E_p(x,t)$ is the classically treated pump field, and $\hat{E}_{NIR}(x,t)$ and $\hat{E}_{IR}(x,t)$ are the signal and idler field operators, respectively. Applying this new Hamiltonian to the output state and expanding it gives us a general form of the two-photon state

$$|\psi\rangle = \int A(\,\omega_{NIR}, \omega_{IR})\, \hat{a}^{\dagger}_{NIR}(\omega_{NIR})\hat{a}^{\dagger}_{IR}(\omega_{IR})|0\rangle_{NIR}|0\rangle_{IR} d\omega_{NIR} d\omega_{IR}.$$

Here, $\hat{a}^{\dagger}_{NIR}(\omega_{NIR})$ and $\hat{a}^{\dagger}_{IR}(\omega_{IR})$ are again the creation operators, but now with explicit frequency dependence. The joint spectral amplitude (JSA), $A(\,\omega_{NIR}, \omega_{IR})$, is approximated by taking the square root of the measured JSI, assuming a constant phase [10]. Generally, the JSA can be described by the product of the two functions detailing the pump envelope and phase matching conditions within the SPDC medium [7]. Tailoring these functions is an important area of research for reducing spectral correlations through source engineering [11, 12]; however, the specific details of such work are outside the scope of this paper.

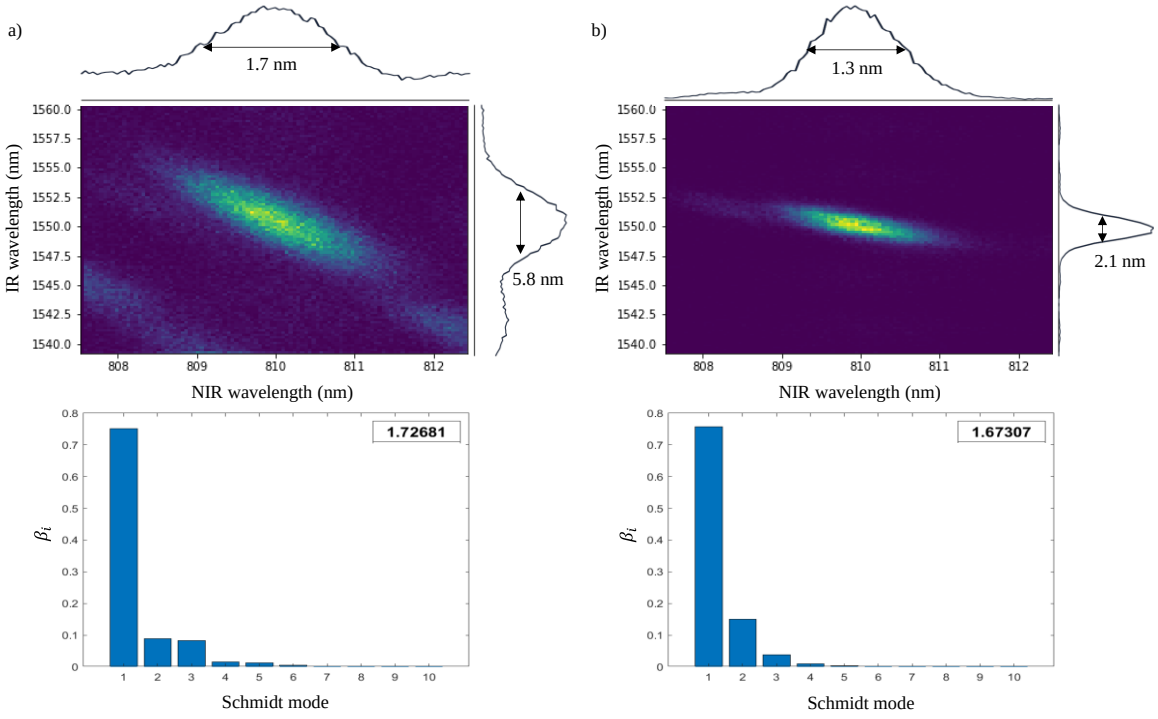

Figure 4: JSIs and Schmidt decompositions for two filter combinations. Also shown are the single-photon spectra with their spectral widths to show effect of the spectral filtering. a) 10 nm (NIR) and 100 nm (IR) spectral bandpass filters. The feature in the lower left corner is due to the NIR spectrum being wider than the limit described in Section 2. This winding also contributes to the higher single photon spectrum background. b) 3 nm (NIR) and 1.8 nm (IR) spectral bandpass filters.

We now quantify the spectral correlations of an entanglement source through an examination of the covariance distribution of the signal and idler photons, a technique known as Schmidt Decomposition, where a pure state, $|\psi\rangle$, describing a two-state system, can be decomposed into orthonormal states. These orthonormal states are the Schmidt modes and are denoted $|i_{NIR}\rangle|i_{IR}\rangle$, for the signal and idler photons, respectively. The Schmidt decomposition is then represented by [13]

$$|\psi\rangle = \sum_i \sqrt{\beta_i} |i_{NIR}\rangle\, |i_{IR}\rangle,$$

where $\sqrt{\beta_i}$ are the Schmidt coefficients satisfying the normalization requirement, $\sum_i \beta_i = 1$. The Schmidt number, K, is a representation of the effective number of modes and is given by

$$K = \frac{1}{\sum_i \beta_i^2}.$$

Figure 4 shows the JSIs and Schmidt coefficients of two combinations of spectral filters applied to the output of the SPDC source. To assess this source's applicability to an entanglement swapping architecture more directly, we consider a related parameter, the spectral purity, P, which is the inverse Schmidt number [7]

$$P = \frac{1}{K}.$$

A near unity spectral purity will be required for efficient entanglement swapping operations, as the spectral purity is directly related to the visibility of a two-source Hong-Ou-Mandel (HOM) interferometer [7]. We calculate P for the two-photon states emitted from our SPDC source under a variety of spectral filter combinations applied to the signal and idler photons. The results are summarized in Table 1, where it is evident that none of the tested spectral filter combinations applied to the presented source result in a sufficiently high spectral purity for entanglement swap-based quantum network architectures. This is due in part to the lack of paired spectral bandpass filters with the correct relative spectral widths. The ideal spectral filter bandwidths are dependent on the unfiltered JSI and central wavelengths of the two photons [7]. Furthermore, spectral filtering alone is, in general, a suboptimal technique for removing unwanted spectral correlations due to the inefficiency of the process and associated loss in otherwise useful quantum resources [14]. What we have shown, however, is the ability of this dual fiber spectrometer, in combination with analytical techniques, to characterize highly non-degenerate entanglement sources of interest.

Table 1: Schmidt number and spectral purity for a variety of spectral bandpass filter combinations applied to the output of the SPDC entanglement source.

NIR Bandpass (nm)	IR bandpass (nm)	*K*	*P*
10	100	1.727	0.579
10	12	1.485	0.673
10	1.8	1.632	0.613
3	100	1.673	0.598
3	12	1.531	0.653
3	1.8	1.741	0.574

4. CONCLUSION

We have demonstrated a dual fiber spectrometer that provides an experimental approach towards understanding the degree of spectral correlation from a quantum transmitter with highly non-degenerate outputs. Sources such as these may prove beneficial as intermediaries between free-space and fiber optic quantum networks. Furthermore, we have developed the tools to quantitatively analyze the measured JSIs, with a focus on spectral purity. As discussed previously, a near unity spectral purity will be required for efficient entanglement swapping operations, as the spectral purity is equivalent to the visibility of a two-source HOM interferometer. In the future, our team will verify and validate our JSI and spectral purity metrologies in combination with in-house developed models and simulations. Specifically, we will use our spectral purity results to extrapolate HOM visibilities, from which we can derive quantum source viability within space-based entanglement swap architectures of interest. Thus, the NASA quantum metrology laboratory will serve as a valuable resource in the understanding of how a wide variety of quantum components may be applicable within future space-based quantum network architectures.

5. ACKNOWLEDGEMENTS

This work was supported by the NASA Space Communications and Navigation (SCaN) program and the Glenn Research Center Communications & Intelligent Systems Division. Research was also sponsored by NASA through a contract with Oak Ridge Associated Universities. The authors would like to thank George Kiriazes, Brady Sites, and Bertram Floyd for their contributions to the work developed in this document.

6. REFERENCES

[1] X.-S. Ma, T. Herbst, T. Scheidl, D. Wang, S. Kropatschek, W. Naylor, B. Wittmann, A. Mech, J. Kofler, E. Anisimova, V. Makarov, T. Jennewein, R. Ursin and A. Zeilinger, "Quantum teleportation over 143 kilometres using active feed-forward," *Nature,* vol. 489, pp. 269-273, 2012.

[2] H. J. Kimble, "The quantum internet," *Nature,* vol. 453, pp. 1023-1030, 2008.

[3] N. Sangouard, C. Simon, H. d. Riedmatten and N. Gisin, "Quantum repeaters based on atomic ensembles and linear optics," *Rev. Mod. Phys.,* vol. 83, no. 33, 2011.

[4] S. Bose, V. Vedral and P. L. Knight, "Multiparticle generalization of entanglement swapping," *Phys. Rev. A,* vol. 57, no. 822, 1998.

[5] R.-B. Jin, M. Takeoka, U. Takagi, R. Shimizu and M. Sasaki, "Highly efficient entanglement swapping and teleportation at telecom wavelength," *Scientific Reports,* vol. 5, no. 9333, 2015.

[6] M. Avenhaus, A. Eckstein, P. J. Mosley and C. Silberhorn, "Fiber-assisted single-photon spectrograph," *Optics Letters,* vol. 34, no. 18, 2009.

[7] K. Zielnicki, K. Garay-Palmett, D. Cruz-Delgado, H. Cruz-Ramirez, M. F. O'Boyle, B. Fang, V. O. Lorenz, A. B. U'Ren and P. G. Kwiat, "Joint Spectral Characterization of Photon-Pair Sources," *Journal of Modern Optics,* vol. 65, no. 10, pp. 1141-1160, 2018.

[8] A. O. C. Davis, P. M. Saulnier, M. Karpinski and B. J. Smith, "Pulsed single-photon spectrometer by," *Optics Express,* vol. 24, no. 11, pp. 12804-12811, 2017.

[9] Coherent, Inc., "780-HP Dispersion," [Online]. Available: http://www.nufern.com/marketing/fiber_data/780-HP_Dispersion.xlsx. [Accessed 02 December 2022].

[10] W. P. Grice and I. A. Walmsley, "Spectral information and distinguishability in type-II down-conversion with a broadband pump," *Physical Review A,* vol. 56, no. 1627, 1997.

[11] C. Chen, J. E. Heyes, K.-H. Hong, M. Y. Niu, A. E. Lita, T. Gerrits, S. W. Nam, J. H. Shapiro and F. N. C. Wong, "Indistinguishable single-mode photons from spectrally engineered biphotons," *Optics Express,* vol. 27, no. 8, 2019.

[12] S. Mittal, V. V. Orre, E. A. Goldschmidt and M. Hafezi, "Tunable quantum interference using a topological source of indistinguishable photon pairs," *Nature Photonics,* vol. 15, pp. 542-548, 2021.

[13] C. K. Law, I. A. Walmsley and J. H. Eberly, "Continuous Frequency Entanglement: Effective Finite Hilbert Space and Entropy Control," *Physical Review Letters,* vol. 84, no. 23, pp. 5304-5307, 2000.

[14] E. Meyer-Scott, N. Montaut, J. Tiedau, L. Sansoni, H. Herrmann, T. Bartley and C. Silberhorn, "Limits on the heralding efficiencies and spectral purities of spectrally filtered single photons from photon-pair sources," *Phys. Rev. A,* vol. 95, 2017.